Heliyon 9 (2023) e18009

Contents lists available at ScienceDirect

Heliyon

journal homepage: www.cell.com/heliyon

ANXA13 promotes cell proliferation and invasion and attenuates apoptosis in renal cell carcinoma

Xiaoyu Niu [a,1], Keyuan Zhao [b,1], Yuanyuan Zheng [c], Yapeng Wang [d], Ruoyang Liu [a], Yiming Zhang [a], Lihui Wang [a], Yongjun Wu [e,f], Xuefeng Bai [f], Baoping Qiao [a,*]

[a] *Department of Urology, The First Affiliated Hospital of Zhengzhou University, Zhengzhou, Henan, 450052, China*
[b] *Department of Urology, Shaoxing People's Hospital, Shaoxing, Zhejiang, 312000, China*
[c] *National Engineering Laboratory for Internet Medical Systems and Applications, First Affiliated Hospital of Zhengzhou University, Zhengzhou, Henan, 450052, China*
[d] *Department of Urology, Daping Hospital, Army Medical University, Chongqing, 404100, China*
[e] *College of Public Health, Zhengzhou University, Zhengzhou, Henan, 450001, China*
[f] *The Key Laboratory of Nanomedicine and Health Inspection of Zhengzhou, Zhengzhou, Henan, 450001, China*

ARTICLE INFO

Keywords:
ANXA13
ccRCC
Proliferation
Invasion and metastasis
Apoptosis

ABSTRACT

Purpose: Emerging evidences have demonstrated that annexin A13 (ANXA13) is closely related to the occurrence and development of malignant tumors. However, the functions and underlying molecular mechanisms of ANXA13 in Clear cell renal cell carcinoma (ccRCC) have not been defined. Therefore, this study aimed to clarify the potential role of ANXA13 in regulating the proliferation, migration, invasion, cell cycle, and apoptosis of ccRCC cells.

Patients and methods: The quantitative real-time PCR (qRT-PCR) and western blotting was performed for detecting the ANXA13 expression in ccRCC tissues at the mRNA and protein levels, respectively. The GEPIA2 databases were used to derive data for analyzing the ANXA13 expression in pan-cancer and ccRCC clinical features. Cell Counting and colony formation assays, as well as flow cytometry, were used to detect cell proliferation, apoptosis, or cell cycle. The wound healing assay was used to evaluate the migration ability of cells, and the *Trans*-well assay was conducted to determine the cell invasiveness.

Results: ANXA13 was upregulated in ccRCC cells and human ccRCC tissues. Furthermore, siANXA13 inhibited ccRCC cell proliferation, migration, invasion and induced cell apoptosis.

Conclusion: ANXA13 was upregulated in ccRCC. ANXA13 promotes tumorigenic traits of ccRCC cell lines *in vitro*. ANXA13 is a potential novel biomarker and a potential therapeutic target in ccRCC.

1. Introduction

Clear cell renal cell carcinoma (ccRCC, kidney renal clear cell carcinoma) accounts for about 80% of renal cancers. It is one of the most common malignant tumors in the urinary system, with an incidence of approximately 2.4% of all malignant tumors in adults. The number of newly diagnosed patients each year exceeds 330,000 [1,2]. The number of patients with ccRCC will increase by

* Corresponding author. Address: No. 1, Jianshe East Road, Zhengzhou, Henan Province, China.
E-mail address: zhangyaling@zzu.edu.cn (B. Qiao).
[1] These authors contributed equally.

https://doi.org/10.1016/j.heliyon.2023.e18009
Received 15 September 2022; Received in revised form 20 June 2023; Accepted 5 July 2023
Available online 22 July 2023

approximately 24.8% in 10 years, and the number of deaths will increase by about 38.6% [3]. At present, the imaging examination accidently detects more than half of ccRCCs [4]. ccRCC has strong metastasis and invasion abilities. At the time of diagnosis, approximately 50% of patients are diagnosed with renal cancers already in the metastatic stages. Approximately 30% patients undergoing early radical nephrectomy still experience distant metastases postoperatively. Different grades and stages of localized kidney Renal Clear Cell Carcinoma (KIRC) are treated with partial nephrectomy and radical nephrectomy [5,6]. Since ccRCC is not sensitive to radiotherapy or chemotherapy, a new generation on targeted therapy and combination immunotherapy currently predominate the advanced and metastatic ccRCC treatment scenario [7–10]. However, previous studies and meta-analyses concluded that the effects of conventional metastatic and advanced ccRCC treatments are average [11]. A study on specific ccRCC gene expression and sensitive ccRCC biomarkers revealed their clinical significance in the diagnosis of ccRCC patients and in accommodating the provision of personalized treatment. Moreover, analysis of the molecular biomarkers of ccRCC has achieved prominence in predicting tumor behavior [12–14].

Annexin A13 (ANXA13), a Ca2+-dependent phospholipid-binding protein member of the polygenic annexin superfamily, plays a role in the regulation of cellular growth and signal transduction pathways [15–17]. The unique, conserved aspects of ANXA13 primary structure and gene organization identify it as the probable common ancestor of all vertebrate annexins [18]. However, the specific function of this gene has not yet been determined. It is postulated to be related to the plasma membrane of undifferentiated proliferating endothelial cells. Limited evidence suggests that ANXA13 may play a role in hypertension [19], apoptosis cell-mediated immunosuppression [20], redundant tolerogenic signals, and cell death recognition [21]. Current studies evidenced that ANXA13 influences the development of lung adenocarcinoma, colorectal cancer, and gastroesophageal junction adenocarcinoma [22–24]. Whereas, relevant reports of its functioning in ccRCC are unavailable. Therefore, this study aimed to clarify the potential role of ANXA13 in regulating the proliferation, migration, invasion, cell cycle, and apoptosis of ccRCC cells.

2. Materials and methods

2.1. Patient and tissue samples

Fifty-six pairs of specimens from 56 patients with ccRCC with matched tumor and para-cancerous (PC) tissues were collected. These tissues were quickly frozen in liquid nitrogen and then stored in a freezer at −81 °C. All patients underwent radical or partial nephrectomy at the First Affiliated Hospital of Zhengzhou University, Henan Province, China between 2018 and 2019. The specific pathological type was confirmed to be renal clear cell carcinoma in the subsequent histopathological diagnosis. All patients were randomly selected and later selected as research subjects. This study was approved by the ethics committee of the First Affiliated Hospital of Zhengzhou University (approval number: 2019-148), and all patients signed an informed consent form for scientific research.

2.2. Databases and bioinformatics

First, we queried the ENSEMBL database (http://asia.ensembl.org/index.html) to identify the ANXA13 gene sequence. Then, we used the GEPIA2 website (http://gepia2.cancer-pku.cn/) based on The Cancer Genome Atlas (TCGA) database to analyze the relative expression difference of the target gene in tumor and PC tissues. The UniProt database (https://www.uniprot.org/) was used to retrieve protein-level information on ANXA13. Global Statistics: The Global Cancer Observatory (GCO, https://gco.iarc.fr/) database is used and the number of newly diagnosed patients includes China.

2.3. Cell lines and culture

Human renal clear cell carcinoma cell lines (ACHN, 786-O, 769-P) and renal normal cell lines (HK-2) were purchased from The Cell Bank of Type Culture Collection of Chinese Academy of Sciences. Cells were cultured in 1640 medium (786-O, 769-P), MEM (minimum essential medium; ACHN), and FK-12 (HK-2) medium (Hyclone, Massachusetts, USA) and were supplemented with 10% fetal bovine serum (FBS) in a humidified atmosphere containing 5% CO_2 at 37 °C (FBS; Gibco; Thermo Fisher Scientific, Inc).

2.4. Construction of siRNA knockdown target gene cell lines

Transient transfection siRNA (siANXA13, sip21, siNC) were provided by GenePharma (GenePharma, Shanghai, China). The ANXA13, MMP9 and Bcl-2 cDNA plasmids (Shanghai GeneChem Co, Ltd., China) were used to upregulate the expression of ANXA13, MMP9 and Bcl-2. The same amount of well-cultured ccRCC cells (ACHN, 786-O, 769-P) was spread in a six-well plate with the complete culture medium. Upon reaching ~50% cell confluence, 200 μL mixed reagent was used per well and 4 μL transfection reagent (Polyplus-transfection®, jetPRIME®, France) was added to the buffer. The mixture was incubated with 5.5 μL of siRNA or cDNA plasmids at room temperature for 10 min and distributed dropwise into the 6-well plate. After 4 h, the transfection was completed. However, we used Fluorescently labelled siNC to verify the transfection efficiency and confirm the transfection of siRNA into cells. The following siRNAs were used in this study including those targeting ANXA13: ANXA13-homo-I, sense 5′-GCUGAACAAAGCCUGCAAATT-3′ and antisense 5′-UUUGCAGGCUUUGUUCAGCTT-3′; ANXA13-homo-II, sense 5′-GCCUCGAAUCAGAUGUCAATT-3′ and antisense 5′-UUGACAUCUGAUUCGAGGCTT-3′; ANXA13-homo-III, sense 5′-CCUUUCAAGCCUAUCAAAUTT-3′ and antisense 5′-AUUUGAUAGGCUUGAAAGGTT-3′; nontargeting controls (si-NC), sense 5′-UUCUCCGAACGUGUCACGUTT-3′ and antisense 5′-

ACGUGACACGUUCGGAGAATT-3′.

2.5. Quantitative real-time polymerase chain reaction (qRT-PCR)

Total RNA and cells were extracted from ccRCC tissues using the TRIzol® reagent (Invitrogen, USA). Total RNA was treated with gDNA remover (Toyobo Life Science) and reverse transcribed into cDNA separately with strand-specific primers using the ReverTra Ace qPCR RT Master Mix (Toyobo Life Science) with the specific conditions according to the manufacturer's protocol [25]. qRT-PCR was performed using an SYBR Green Mix (Roche Diagnostics) and a QuantStudio 3 Real-Time PCR System (Thermo Fisher Scientific, Inc.) in a 20 μL reaction mixture using the specific conditions for analysis. The following primer pairs were used for the qRT-PCR: ANXA13 forward, 5′ CAGGGCAATAGGAACACAGGG-3′ and reverse, 5′ GGTTTTCGTGCGGGAGTCT-3′; GAPDH forward, 5′ CAGGAGGCATTGCTGATGAT-3′ and reverse,

5′-GAAGGCTGGGGCTCATTT-3′. Relative expression was normalized to the internal reference gene GAPDH using the $2^{-\Delta\Delta Ct}$ method.

2.6. Western blotting

Tissue specimens and cells were lysed with a radio-immunoprecipitation assay buffer (Solarbio Life Sciences, Shanghai, China), and the protein concentrations were determined using the bicinchoninic acid protein assay kit (EpiZyme, Shanghai, China). Protein samples (30 μg/lane) were separated by sodium dodecyl sulfate-polyacrylamide gel electrophoresis on 12.5% gels and transferred onto polyvinylidene fluoride membranes. The membranes were blocked with 10% skim milk for 2 h at room temperature and then incubated with primary antibodies against ANXA13 (ab151517; Abcam, USA), P21 (AP021; Beyotime Institute of Biotechnology, China), Cyclin B1 (AF1606; Beyotime Institute of Biotechnology, China), MMP2 (GB111507; Servicebio , China) , MMP9 (GB12132-1; Servicebio , China) , Bax (2774; CST , USA) , Bak (12105; CST , USA) , Bcl-2 (15071; CST , USA) , Caspase-3 (9662; CST , USA) , Cleaved Caspase-3 (9661; CST , USA) , PARP (9532; CST , USA) , Cleaved PARP (5625; CST , USA) , Actin (GB12001; Servicebio , China) , and GAPDH (AP0063; Bioworld Technology, USA) at 4 °C overnight. Following primary antibody incubation, the membranes were incubated with anti-rabbit horseradish peroxidase secondary antibody (A21020; Abbkine Scientific Co., Ltd, China) and anti-mouse horseradish peroxidase secondary antibody (A21010, Abbkine Scientific Co., Ltd, China) at room temperature for 1 h. Protein bands were subsequently visualized using enhanced chemiluminescence reagent kits (Millipore Corporation, Billerica, USA) and scanned with an imaging system (Bio-Rad Laboratories, Inc). Protein densitometry was quantified using Image J software v1.8.0.

2.7. Cell counting Kit-8 (CCK-8) assay

Cell proliferation ability was determined using the CCK-8 (Dojindo Laboratories, Japan). Transfected siNC and siANXA13 cells were seeded on 96-well plates and incubated for 24, 36, 48, and 72 h at 37 °C. Absorbance was measured by adding 10 μL of CCK-8 reagent to each well and incubating them in the dark for 2 h, and absorbance was measured at 450 nm.

2.8. Colony formation assays

Colony formation assays were performed to monitor the ccRCC cloning capability of stable knockdown of ANXA13. The transfected siNC and siANXA13 cells were seeded in 6-well plates at approximately 1000 cells per well. ACHN and 786-O cells cultured for 15 and 12 days, respectively, were fixed and stained, and colonies were fixed with 4% fixative solution (Solarbio Life Sciences, Beijing, China) and stained with 0.1% crystal violet staining solution. Each well was washed with water and then photographed, and Image J software was used for cell counting.

2.9. Flow cytometry

Cell cycle inhibition was determined using the Cycle Test Plus DNA Reagent Kit (BD Biosciences Pharmingen, Franklin Lakes, NJ, USA), according to the manufacturer' s instructions. The treated cells were collected 48 h after transfection and washed twice with phosphate buffer solution (PBS). The cells were fixed with ice-cold 70% ethanol and incubated at −20 °C overnight. Subsequently, the fixed cells were washed twice with PBS and incubated with 200 μL propidium iodide (PI) solution with RNaseA (BD Biosciences Pharmingen, Franklin Lakes, NJ, USA) at room temperature for 30 min in the dark. The treated cells were subsequently analyzed using the NovoCyte Flow Cytometer (ACEA Biosciences, Inc, San Diego, CA, USA) with NovoExpress® software (1.3.0; ACEA Biosciences, Inc, San Diego, CA, USA, 2018). Early and late apoptotic cells were analyzed using the Annexin V-FITC Apoptosis Detection Kit I (BD Biosciences Pharmingen, Franklin Lakes, NJ, USA). The cells were trypsinized without ethylenediamine tetraacetic acid and scraped twice with cold PBS. Subsequently, the cells were stained using the Annexin V-FITC/PI kit at room temperature for 30 min in the dark according to the manufacturer's protocol. The treated cells were analyzed by the procedure used for the cell cycle analysis.

2.10. Cell invasion assay

The 786-O and ACHN cells were digested and dispersed into serum-free 1640 medium and MEM with a density of 1×10^6 cells/mL. Cell invasion abilities were detected using the Transwell assay. Matrigel and serum-free medium were mixed (1:8), spread in a small

chamber, and incubated at 37 °C overnight in a 5% CO_2 atmosphere. Subsequently, 200 μL cell suspension was inoculated into 24-well Transwell chambers with a polycarbonate membrane (8.0 μm pore size). Complete medium (1 ml, 10% FBS) was added to the bottom of each well. After 24 h incubation, the cells at the bottom of the polycarbonate membrane were fixed, stained, and counted.

2.11. Cell migration assay

The migration ability of the cells was analyzed by a wound healing assay. In this assay, 1×10^6 siANXA13 cells or siNC cells were seeded on six-well plates, incubated for 24/48 h, washed with a pipette tip, and washed thrice with PBS. The plates were imaged by a digital camera at 0 and 24 h for comparison.

2.12. TUNEL assay

TUNEL assay was performed by using riboAPO One-Step TUNEL Apoptosis kit (RiboBio, Guangzhou, China) according to the manufacturer's instructions. Briefly, apoptotic cells were fixed by 4% formaldehyde for 15 min at room temperature. Then, the cells were permeabilized by 0.5% TritonX-100 for 10 min. Cells were labelled with 50 μL TdT reaction mix at 37 °C for 2 h. SSC buffer was used to stop the reaction and stained nuclei with DAPI. The images were photographed by an Olympus FSX100 microscope (Olympus,

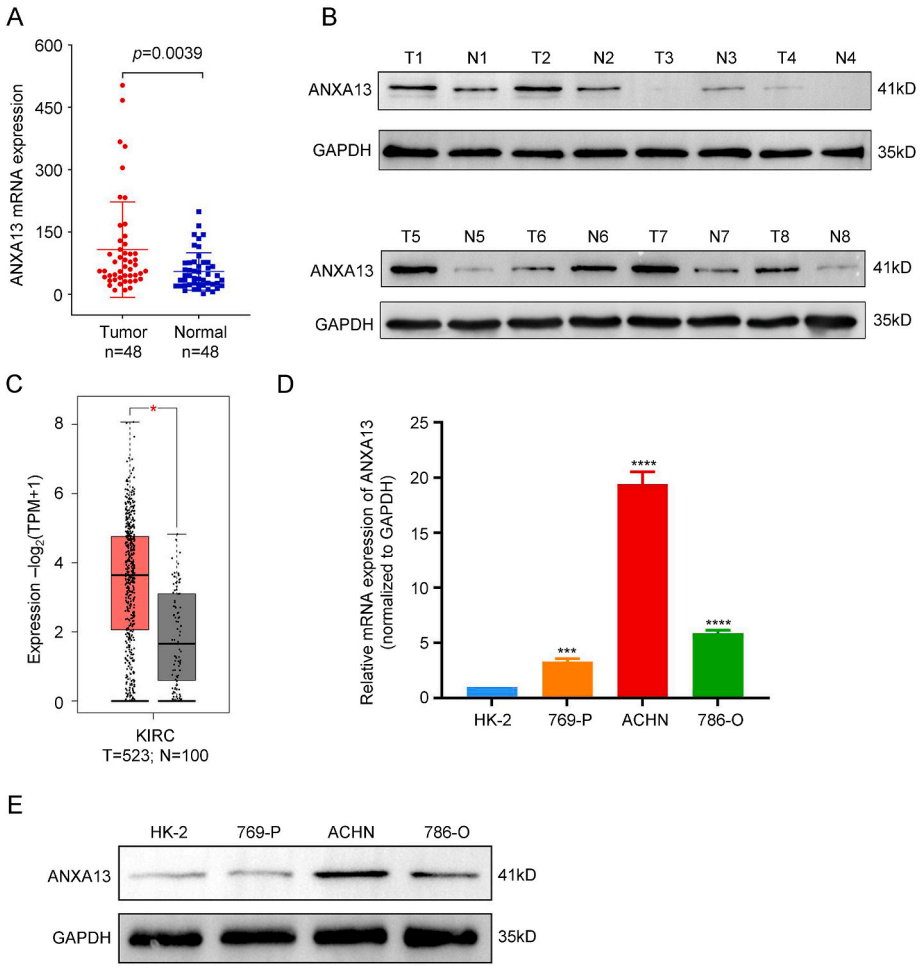

Fig. 1. ANXA13 is upregulated in human ccRCC tissues. (A) The expression of ANXA13 in human ccRCC tissues (n = 48) and PC tissues (n = 48) were determined by reverse transcription-quantitative PCR, normalized to GAPDH and analyzed by the paired samples *t*-test. (B) Upregulated expression of the ANXA13 protein was observed in 6/8 ccRCC cases using Western blot when compared to the PC tissues. T, ccRCC tissue; N, PC tissue. Use Image J software to analyze protein bands for grayscale analysis, and normalize the grayscale values of the target protein before using GraphPad Prism software for statistical analysis. (C) The expression of ANXA13 in human KIRC tissues (n = 523) and PC tissues (n = 100) from the GEPIA2 database. (D) mRNA expression of ANXA13 in the ccRCC cell lines 786-O, ACHN and 769-P and normal cell line HK2, normalized to GAPDH and analyzed by the Bonferroni's post hoc test. (E) Protein level of ANXA13 in the ccRCC cell lines 786-O, ACHN, and 769-P and normal cell line HK-2. ****p < 0.0001, ****p < 0.0001, ***p < 0.001, *p < 0.05. All data were representative of at least three independent experiments (n = 3; error bar, SD).

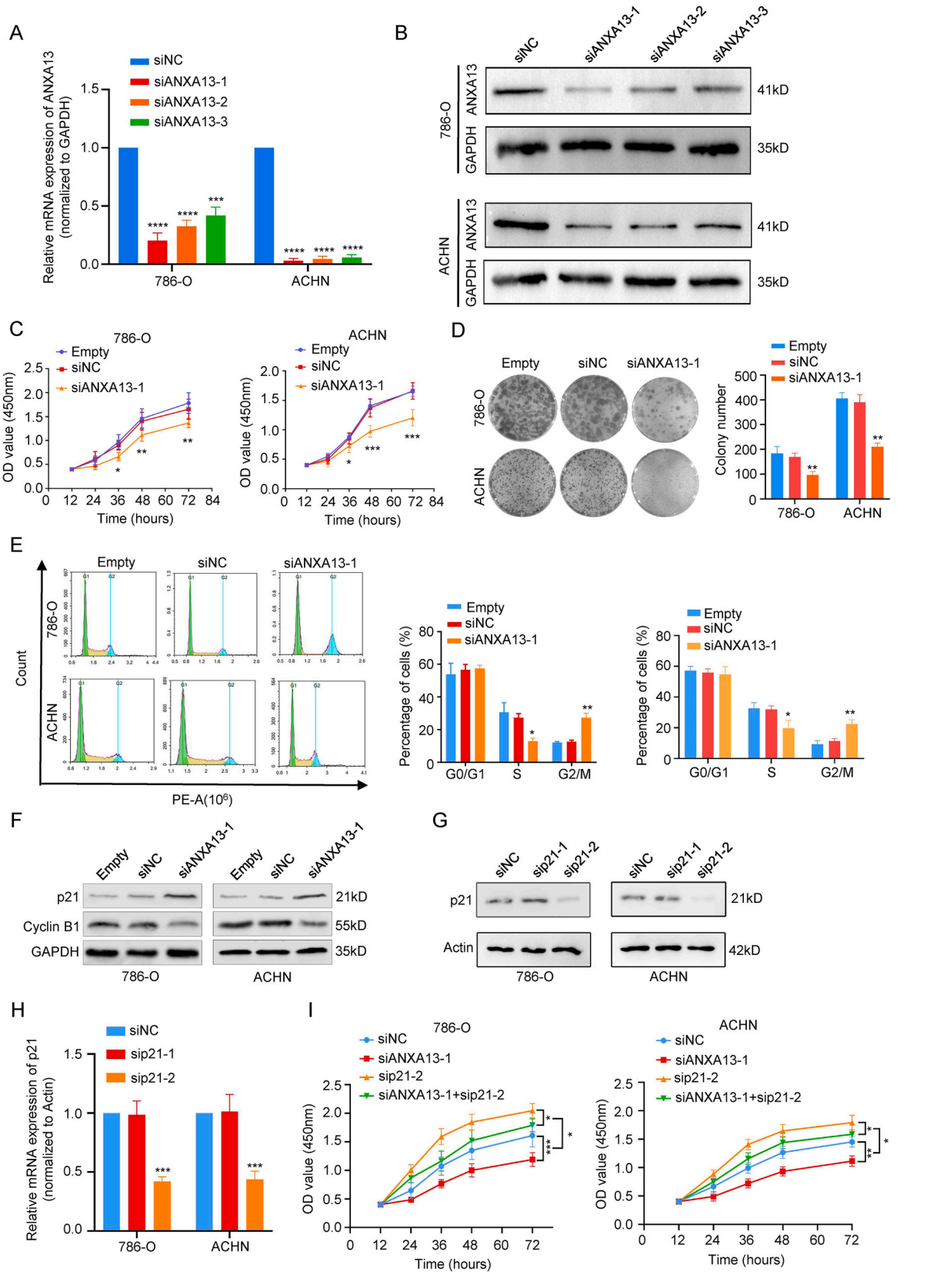

(caption on next page)

Fig. 2. Knockdown of ANXA13 represses the proliferation of ccRCC cells. (A and B) The knockdown effect of three siANXA13 was detected by qRT-PCR and western blotting assay. (C) The Cell Counting Kit-8 assay was performed to investigate the proliferation of ccRCC cell lines that were either untreated or transfected with siNC or siANXA13. (D) Efficacy of siANXA13 on colony formation of ccRCC cells. Unpaired Student's t-test was used for data analysis. (E) SiANXA13 triggered G2/M cell cycle arrest in ccRCC cells. Cell cycle distribution of ACHN and 786-O cells that were either untreated or treated with siNC or siANXA13 for 48 h, followed by PI staining and analyzed using flow cytometry for cell cycle profile. Distribution was analyzed by Modified and Graphpad software. (F) Effect of siANXA13 on the expression of cell-cycle-related proteins. GAPDH was used as a loading control. (G and H) Knockdown effect of two sip21 was detected by western blotting assay and qRT-PCR. Actin was used as a loading control. (I) Cell proliferation ability in siNC group, siANXA13-1 group, sip21-2 group and siANXA13-1+sip21-2 group were presented by Cell Counting Kit-8. Unpaired Student's t-test was used for data analysis. ****$p < 0.0001$, ***$p < 0.001$, **$p < 0.01$, *$p < 0.05$. All data were representative of at least three independent experiments ($n = 3$; error bar, SD).

Japan).

2.13. Statistical analysis

Data are presented as means ± standard deviations of three independent experiments. Paired or unpaired Student's t-test were used to compare differences between two groups, when the variables were normally distributed, unpaired Student's t-test was used to compare two groups and one-way ANOVA was used to compare multiple groups, followed by Bonferroni's post hoc test. SPSS was used for data normality test, and Kolmogorov-Smirnov test was used for calculation when the data volume was greater than 50. When the data amount is less than 50, use the Shapiro-Wilk test. When $p > 0.05$, the data obeyed normal distribution. The Fisher's exact test was used to analyze the association between ANXA13 expression and clinicopathological variables in ccRCC. The χ^2 test or Fisher's exact test was used appropriately to identify significant associations between the categorical variables of the two groups. Statistical analyses were performed using GraphPad Prism software (version 7.0; GraphPad Software, Inc.), and the baseline data of the patients were analyzed using SPSS 26.0 software (Alteryx, USA). $p < 0.05$ was considered statistically significant.

3. Results

3.1. Abnormal high expression of ANXA13 in ccRCC cells and samples

We evaluated the expression of ANXA13 in tumor and PC tissues of 48 paired specimens from patients with ccRCC by qRT-PCR analysis, which revealed the upregulation of ANXA13 transcription in tumor tissues ($p = 0.0039$) (Fig. 1A). The protein expression of ANXA13 was evaluated in eight pairs of tumor and PC tissues through Western blotting. Higher ANXA13 expression was found in 6/8 ccRCC tissues ($p = 0.02$) (Fig. 1B). Consistently, we found the same result by analysis the data from the GEPIA2 database (Fig. 1C) [26]. Besides, we found the higher expression levels of both ANXA13 mRNA and protein in three human ccRCC cell lines (ACHN, 786-O, 769-P) as compared with normal renal cell line (HK-2) (Fig. 1D and E). These results indicated that ANXA13 might promote ccRCC progression. However, we found that an unexpected small number of patients with a high grade ccRCC (Grade III-IV) showed a low ANXA13 expression (Table S1).

3.2. Knockdown of ANXA13 represses the proliferation of ccRCC cells through increasing the expression of p21 and decreasing the expression of cyclin B1

Next, we selected 786-O and ACHN, two types of tumor cells with relatively high expression, as the further research objects. The mRNA and protein expression levels of ANXA13 were detected using three types of siANXA13-transfected cells and the negative control siNC-transfected cells. Meanwhile, fluorescently labelled siNC was transfected into ACHN and 786-O cells and recorded, and the fluorescence expression of green fluorescent protein was photographed in the transfected cells (Figure S1A), confirming that the 786-O and ACHN cell lines were successfully transfected. We finally selected siANXA13-1 for further studies because of its obvious knockdown effects (Fig. 2A and B).

The effect of ANXA13 expression on cell proliferation was evaluated using the CCK-8 assay. The assay data showed that compared with the control cells, ANXA13 knockdown significantly decreased the proliferation rate in 786-O and ACHN cells at 36, 48, and 72 h after transfection (Fig. 2C). The tumorigenicity evaluation of ACHN and 786-O cells transfected with siANXA13 by colony formation assay showed a significantly reduced number of newly formed colonies in the siANXA13 transfection group than that of the control group, and the colony formation ability was impaired (Fig. 2D). Similarly, we found that overexpression of ANXA13 promotes 786-O and ACHN cells proliferation (Figure S2A-C).

To elucidate the growth suppression mechanism of siANXA13, the cell cycle profile was examined after treatment with siANXA13, which induced G2/M cell cycle arrest (Fig. 2E). The expression of cell cycle-related proteins was further examined by western blotting. Results showed that siANXA13 treatment increased the protein level of p21 and decreased the expression of Cyclin B1 (Fig. 2F), implying that siANXA13 treatment caused G2 phase cell cycle arrest. We found the same result in the ANXA13 overexpression group (Figure S2D). Importantly, the inhibitory effects of siANXA13 on ccRCC cell proliferation were partly reversed upon knockdown of p21 (Fig. 2G–I).

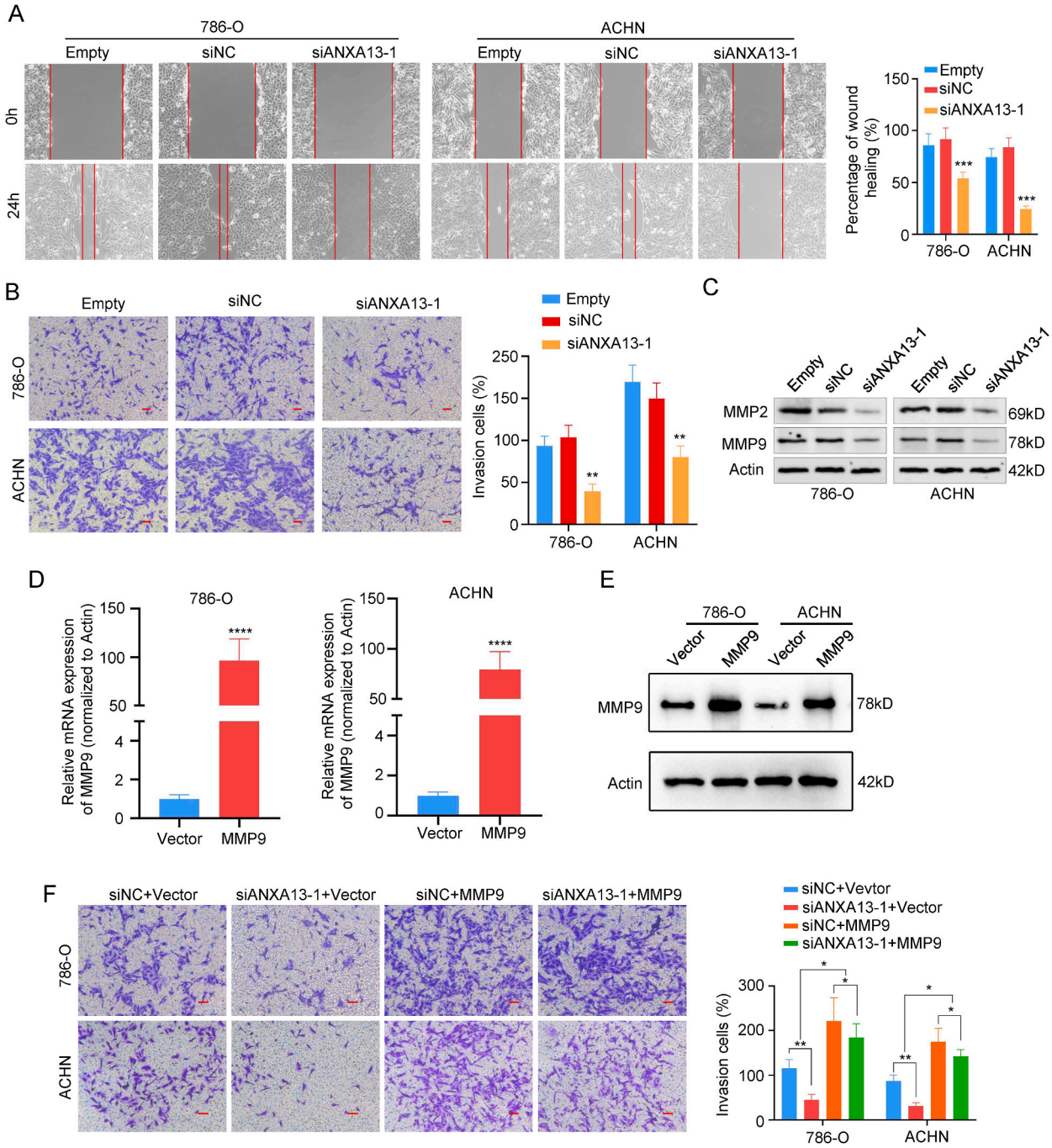

Fig. 3. SiANXA13 inhibits ccRCC cell migration and invasion. (A) Wound healing assays were performed in 786-O and ACHN cells that were either untreated or treated with siNC or siANXA13. (B) The invasion ability of ACHN and 786-O cells was evaluated using *Trans*-well analysis. Scale bar: 50 μm. (C) Western blotting shows that MMP2/MMP9 proteins changed in response to ANXA13 knockdown. Actin was used as a loading control. (D and E) The expression of MMP9 were tested by qRT-PCR or Western blotting after transfected with MMP9 cDNA plasmids or empty cDNA vector. Actin was used as a loading control. (F) After co-transfection with MMP9 cDNA plasmids or siANXA13, *Trans*-well analysis was used to evaluate the invasion ability of ACHN and 786-O cells. Scale bar: 50 μm. Unpaired Student's t-test was used for data analysis. ****$p < 0.0001$, ***$p < 0.001$, **$p < 0.01$, *$p < 0.05$. All data were representative of at least three independent experiments ($n = 3$; error bar, SD).

3.3. Knockdown of ANXA13 reduces the invasion and migration ability of ccRCC cells through decreasing the expression of MMP2 and MMP9

The wound healing assay was used to evaluate the migration ability of the cells. Compared with the siNC group, a wider wound and weaker cell migration were observed in the siANXA13-transfected group (Fig. 3A). The invasion ability of ACHN and 786-O cells was evaluated using *Trans*-well analysis. Compared with the siNC group, the number of invasive cell lines in the siANXA13 group was significantly reduced (Fig. 3B). Simultaneously, we found that overexpression of ANXA13 promotes 786-O and ACHN cells migration and invasion (Figure S2E-F). The result from western blotting showed that depletion of ANXA13 remarkably reduced the expression of MMP2/MMP9, which mediate cell migration and invasion, respectively (Fig. 3C). We also found that up-expression of ANXA13 remarkably promoted the protein expression of MMP2 and MMP9 in 786-O and ACHN cells (Figure S2G). Moreover, ectopic expression of MMP9 partly reversed the inhibitory effects of siANXA13 on ACHN and 786-O cells invasion ability (Fig. 3D–F). Considering these findings, ANXA13 plays a potentially crucial role in the invasion and migration of ccRCC cells.

3.4. Downregulation of ANXA13 promotes ccRCC cell apoptosis

SiANXA13-transfected 786-O and ACHN cells were verified for apoptotic changes using flow cytometry. We found that compared with the siNC group, the proportion of apoptosis in the siANXA13 group increased (Fig. 4A). As well, TUNEL assay showed that ANXA13 knockdown in ACHN and 786-O cells significantly promoted cell apoptosis (Fig. 4B). To confirm our findings, we analyzed protein levels of Bax/BAK/Bcl-2, caspase-3/Cleaved caspase-3, and PARP/Cleaved PARP by Western blotting. The results showed that compared with the control group, Bax/BAK Cleaved caspase-3, and Cleaved PARP expressions were significantly increased in the siANXA13 group, while Bcl-2, caspase-3, and PARP expression levels were downregulated (Fig. 4C). Besides, the increased effects of siANXA13 on 786-O and ACHN cells apoptosis were partly reversed upon overexpression of Bcl-2 (Fig. 4D–F). These findings emphasize that the downregulation of ANXA13 remarkably promoted cell apoptosis.

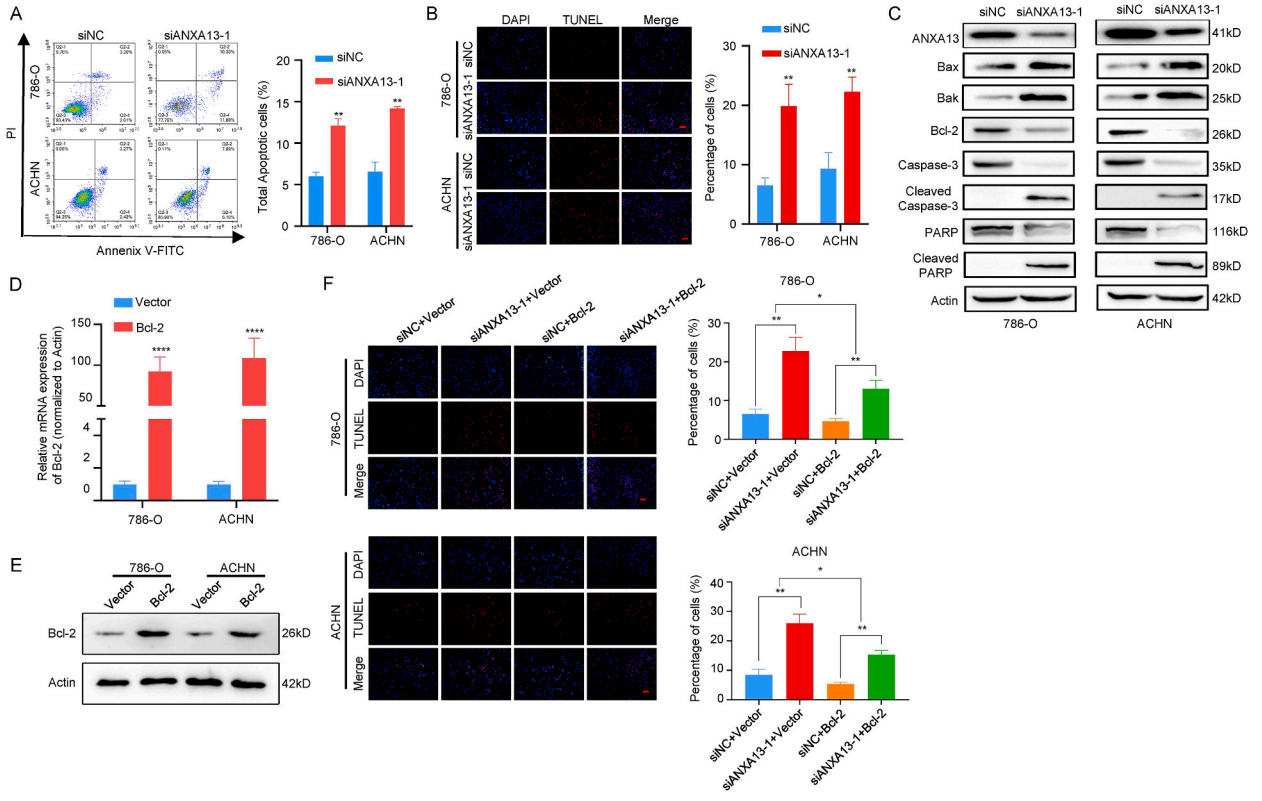

Fig. 4. SiANXA13 induces ccRCC cell apoptosis. (A) Apoptotic cell death of 786-O and ACHN cells treated with siNC or siANXA13 for 48 h and analyzed by flow cytometry using Annexin V-FITC/PI double-staining kit. Annexin V+ cell populations were defined as apoptosis. (B) TUNEL staining analysis of cell apoptosis. Scale bar: 100 μm. (C) Western blotting shows that Bax/Bak/Bcl-2/Caspase-3/Cleaved Caspase-3/PARP/Cleaved PARP proteins changed in response to ANXA13 knockdown. (D and E) The expression of Bcl-2 was tested by qRT-PCR or Western blotting after transfected with Bcl-2 cDNA plasmids or empty cDNA vector. Actin was used as a loading control. (F) Cell apoptosis in siNC + vector group, siANXA13-1+vector group, siNC + Bcl-2 group and siANXA13-1+ Bcl-2 group were presented by TUNEL staining analysis. Scale bar: 100 μm. Unpaired Student's t-test was used for data analysis. $^{**}p < 0.01$, $^{*}p < 0.05$. All data were representative of at least three independent experiments (n = 3; error bar, SD).

4. Discussion

Late tumor and metastasis are the leading causes for the high mortality rates of ccRCC. Investigating the molecular pathogenesis for ccRCC progression and developing new therapeutic strategies for ccRCC are crucial. Previous studies showed that overexpression or knockdown of ANXA13 can effectively inhibit lung adenocarcinoma and colorectal cancer cell proliferation, invasion, and migration [22–24,27,28]. ANXA13 has been reported to be specifically expressed in gastroesophageal junction adenocarcinomas through genomic array analysis [24]. However, whether ANXA13 knockout in ccRCC can significantly inhibit the growth of ccRCC cells is unclear. In our experiments, we found that the expression of ANXA13 in the tumor tissues of patients with ccRCC was relatively higher than that in the normal adjacent tissues and was reverified using data from the TCGA database. We also found that knockdown of ANXA13 and treatment could significantly inhibit the proliferation, migration, and invasion of ccRCC cells, as well as effectively inhibit the growth of ccRCC cells by inducing G2/M cell cycle arrest and apoptosis. Here, our results indicate that siANXA13 treatment effectively suppressed ccRCC cell growth by inducing G2/M cell cycle arrest and apoptosis. Treatment of ANXA13 increased the protein level of p21, Bax, Bak, Cleaved Caspase-3, and Cleaved PARP. However, it reduced the protein levels of cyclin B1, MMP2, MMP9, Bcl-2, Caspase-3, and PARP. This implies that siANXA13 significantly inhibited the proliferation, migration, invasion, and apoptosis of ccRCC cells.

The expression levels of proteins in tumors vary during different stages of tumor development, depending on the type of tumor and the specific protein. For example, some anti-tumor proteins, such as p53, BRCA1, and PTEN, are highly expressed in early stages of the tumor and can inhibit the proliferation and growth of tumor cells [29–31]. However, their expression levels may decrease in later stages, leading to further tumor deterioration [31]. On the other hand, some proteins that promote tumor development have different expression levels at different stages of the tumor. For instance, the HER2 protein is expressed at low levels in early breast cancer, but significantly increases in later stages, making it one of the targets for treating breast cancer [32]. In this study, we found that ANXA13 was significantly higher in ccRCC tissues smaller than 5 cm compared with NC tissue, but this difference disappeared in tumor tissue larger than 5 cm (Table S1). In addition, we found that an unexpected small number of patients with a high grade ccRCC (Grade III-IV) showed a low ANXA13 expression (Table S1). Tumor heterogeneity, characterized by differences in genotype and phenotype among patients with the same type of malignant tumor, as well as within different regions of the same patient's tumor, is a critical feature of malignant tumors [33]. Clear cell renal cell carcinoma (ccRCC) is a prime example of tumor heterogeneity that leads to poor clinical responses among patients, thereby adding to the challenge of treatment [34]. Our study revealed that ANXA13 is highly expressed in most renal cell carcinoma tissues and low expressed in a small portion of ccRCC tissues, thus providing evidence of the tumor heterogeneity in renal ccRCC. However, the small sample size used in our study may have influenced the conclusion. Thus, we plan to increase the sample size in future studies to validate our findings. Overall, the opposite expression patterns of proteins in different stages of tumors are common, which also illustrates the complexity and diversity of tumor development.

A large amount of evidence shows that patients with advanced and metastatic ccRCC are not sensitive to radiotherapy and chemotherapy [7–9]. In recent years, targeted therapy related to drugs with targeted gene silencing siRNA has become a hot topic in research and treatment [35,36]. RNAi is a powerful tool for target identification and provides an alternative therapeutic method to small-molecule and antibody-based therapeutics for inhibiting gene function. In emerging technologies and anti-cancer therapies, small interfering RNA (siRNA) and RNA interference (RNAi) are recognized to silence all genes that may lead to regulation or targeted blocking of biological processes, which are the defining hallmarks of cancer [37,38]. Therefore, RNAi is expected to pave the way for cancer treatment [39].

The cell cycle is a complex process that involves numerous regulatory factors. Any toxin or drug with DNA damaging ability is expected to alter cell cycle progression [40]. Several therapeutic drugs, such as DNA-damaging drugs, topoisomerase inhibitors, antimetabolites and microtubule inhibitors, take advantage of this disruption in normal cell cycle regulation and ultimately induce tumor cell growth arrest or apoptosis. P21, the apoptosis and cell cycle regulatory protein, can also act as a cell cycle inhibitor [41,42]. Cyclin B1 is closely related to the G2/M phase, and its mRNA expression level reaches its peak in this phase [43]. Matrix metalloproteinases (MMPs) play a critical role in the metastasis and invasion of KIRC. MMP2 and MMP9 are major MMPs implicated in cancer progression that degrade the extracellular matrix components [44,45]. Apoptosis is regulated by varied factors and regulatory pathways, including the mitochondrial pathway, which is an important endogenous pathway of apoptosis. The key proteins of the mitochondrial pathway, such as Bax/BAK/Bcl-2 and Caspase-3, have key functions in causing apoptosis [46]. By delving into the mechanism of these apoptosis-inducing proteins, we can better understand the process of tumor cell apoptosis.

In summary, we found that ANXA13 was upregulated in ccRCC cells and human ccRCC tissues. Moreover, stable interference of ANXA13 expression suppressed ccRCC cell proliferation, migration and invasion, while it could change the cell cycle and promote apoptosis. However, the high expression of ANXA13 needs to be reproduced and analyzed in a larger sample of patients in the future. Additional *in vivo* studies and rescue experiments are warranted to confirm that ANXA13 regulation helps suppress cell function. Finally, we will investigate the mechanisms and related pathways of ANXA13 to identify specific markers and targets for the diagnosis and treatment of ccRCC in future studies.

5. Conclusions

The knockdown of ANXA13 can affect cell cycle and apoptosis by regulating p21/cyclin B1 and Bax/Bak/Bcl-2/Caspase-3/Cleaved Caspase-3/PARP/Cleaved PARP proteins. It can also inhibit the migration and invasion of ccRCC cells by regulating MMP2/MMP9 proteins. This study provides a foundation for further preclinical evaluations. ANXA13 may serve as a novel biomarker and a potential anticancer agent in the treatment of ccRCC.

Author contribution statement

Xiaoyu Niu: Keyuan Zhao: Conceived and designed the experiments; Performed the experiments; Wrote the paper.
Yuanyuan Zheng: Yapeng Wang: Analyzed and interpreted the data.
Ruoyang Liu: Yiming Zhang: Yongjun Wu: Xuefeng Bai: Performed the experiments.
Lihui Wang: Contributed reagents, materials, analysis tools or data.
Baoping Qiao: Conceived and designed the experiments; Wrote the paper.

Acknowledgments

This study was funded by the National Natural Science Foundation of China (81973099, 82273685), and the Key Technology Research and Development Program of He'nan Educational Committee (202102310447).

Data availability statement

Data included in article/supp. material/referenced in article.

Availability of data and materials

We agree to make all data available after publication. The following is how to obtain the relevant database.
The Ensembl database (http://asia.ensembl.org/index.html);
The GEPIA2 website (http://gepia2.cancer-pku.cn/);
The UniProt database (https://www.uniprot.org/).

Declaration of competing interest

The authors declare that they have no known competing financial interests or personal relationships that could have appeared to influence the work reported in this paper.

Appendix A. Supplementary data

Supplementary data related to this article can be found at https://doi.org/10.1016/j.heliyon.2023.e18009.

Abbreviations

ccRCC	Clear Cell Renal Cell Carcinoma
KIRC	kidney Renal Clear Cell Carcinoma
ANXA1-11,13	annexin A1-11,13; PC,para-cancerous
TCGA	the Cancer Genome Atlas; GTEx, Genotype-Tissue Expression
GEPIA	Gene Expression Profiling
PARP	poly (ADP ribose) polymerase
BLCA	Bladder Urothelial Carcinoma
BRCA	Breast invasive carcinoma; CESC Cervical squamous cell carcinoma and endocervical adenocarcinoma
CHOL	Cholangiocarcinoma
COAD	Colon adenocarcinoma
ESCA	Esophageal carcinoma
GBM	Glioblastoma multiforme
GBMLGG	Glioma; HNSC Head and Neck squamous cell carcinoma
KICH	Kidney Chromophobe; KIRP Kidney renal papillary cell carcinoma
LIHC	Liver hepatocellular carcinoma
LUAD	Lung adenocarcinoma
LUSC	Lung squamous cell carcinoma
PAAD	Pancreatic adenocarcinoma
PRAD	Prostate adenocarcinoma
PCPG	Pheochromocytoma and Paraganglioma; READ Rectum adenocarcinoma
SARC	Sarcoma; SKCM Skin Cutaneous Melanoma
THCA	Thyroid carcinoma
THYM	Thymoma
STAD	Stomach adenocarcinoma
UCEC	Uterine Corpus Endometrial Carcinoma

References

[1] F. Bray, J. Ferlay, I. Soerjomataram, R. L Siegel, L. A Torre, A. Jemal, Global cancer statistics 2018: GLOBOCAN estimates of incidence and mortality worldwide for 36 cancers in 185 countries, Ca - Cancer J. Clin. 68 (6) (2018) 394–424.
[2] R.J. Motzer, et al., Kidney cancer, version 2.2017, NCCN Clinical Practice Guidelines in Oncology 15 (6) (2017) 804–834.
[3] L. Wu, X. Qu, Cancer biomarker detection: recent achievements and challenges, Chem. Soc. Rev. 44 (10) (2015) 2963–2997.
[4] B. Ljungberg, et al., European association of urology guidelines on renal cell carcinoma: the 2019 update, Eur. Urol. 75 (5) (2019) 799–810.
[5] B. Escudier, et al., Renal cell carcinoma: ESMO Clinical Practice Guidelines for diagnosis, treatment and follow-up, Ann. Oncol. 30 (5) (2019) 706–720.
[6] M.P. Laguna, Re: partial nephrectomy versus radical nephrectomy for clinical T1b and T2 renal tumors: a systematic review and meta-analysis of comparative studies, J. Urol. 198 (6) (2017) 1204–1206.
[7] B.D. Curti, Immunotherapy in advanced renal cancer - is cure possible? N. Engl. J. Med. 378 (14) (2018) 1344–1345.
[8] P.C. Barata, B.I. Rini, Treatment of renal cell carcinoma: current status and future directions, Ca - Cancer J. Clin. 67 (6) (2017) 507–524.
[9] C. Porta, M. Schmidinger, Renal cell carcinoma treatment after first-line combinations, Lancet Oncol. 20 (10) (2019) 1332–1334.
[10] J. Qiu, et al., Therapeutic effect and adverse reaction of sorafenib in the treatment of advanced renal cancer, Oncol. Lett. 17 (2) (2019) 1547–1550.
[11] N. Singla, A new therapeutic era for metastatic renal cell carcinoma: call for a new prognostic model, JAMA Oncol. 6 (5) (2020) 633–634.
[12] J. Graham, S. Dudani, D.Y.C. Heng, Prognostication in kidney cancer: recent advances and future directions, J. Clin. Oncol. (2018), JCO2018790147.
[13] A. Cimadamore, et al., Biomarkers of aggressiveness in genitourinary tumors with emphasis on kidney, bladder, and prostate cancer, Expert Rev. Mol. Diagn 18 (7) (2018) 645–655.
[14] S.F. Shariat, E. Xylinas, Biomarkers in personalised treatment of renal-cell carcinoma, Lancet Oncol. 13 (8) (2012) 751–752.
[15] V. Gerke, S.E. Moss, Annexins: from structure to function, Physiol. Rev. 82 (2) (2002) 331–371.
[16] G.L. Xue, C. Zhang, G.L. Zheng, L.J. Zhang, J.W. Bi, Annexin A13 predicts poor prognosis for lung adenocarcinoma patients and accelerates the proliferation and migration of lung adenocarcinoma cells by modulating epithelial-mesenchymal transition, Fundam. Clin. Pharmacol. 34 (6) (2020) 687–696.
[17] B. Linke, et al., The tolerogenic function of annexins on apoptotic cells is mediated by the annexin core domain, J. Immunol. 194 (11) (2015) 5233–5242.
[18] J. Turnay, E. Lecona, S. Fernández-Lizarbe, A. Guzmán-Aránguez, M.P. Fernández, N. Olmo, Maria Antonia Lizarbe, Structure-function relationship in annexin A13, the founder member of the vertebrate family of annexins, Biochem. J. 389 (2005) 899–911.
[19] K. Kinoshita, M.S. Ashenagar, M. Tabuchi, H. Higashino, Whole rat DNA array survey for candidate genes related to hypertension in kidneys from three spontaneously hypertensive rat substrains at two stages of age and with hypotensive induction caused by hydralazine hydrochloride, Exp. Ther. Med. 2 (2) (2011) 201–212.
[20] B. Linke, et al., The tolerogenic function of annexins on apoptotic cells is mediated by the annexin core domain, J. Immunol. 194 (11) (2015) 5233–5242.
[21] S. Rosenbaum, et al., Identification of novel binding partners (annexins) for the cell death signal phosphatidylserine and definition of their recognition motif, J. Biol. Chem. 286 (7) (2011) 5708–5716.
[22] G. Jiang, P. Wang, W. Wang, W. Li, L. Dai, K. Chen, Annexin A13 promotes tumor cell invasion in vitro and is associated with metastasis in human colorectal cancer, Oncotarget 8 (13) (2017) 21663–21673.
[23] G.L. Xue, C. Zhang, G.L. Zheng, L.J. Zhang, J.W. Bi, Annexin A13 predicts poor prognosis for lung adenocarcinoma patients and accelerates the proliferation and migration of lung adenocarcinoma cells by modulating epithelial-mesenchymal transition, Fundam. Clin. Pharmacol. 34 (6) (2020) 687–696.
[24] M. Duin, R. Marion, K.J. Vissers, W.C.J. Hop, W.N.M. Dinjens, H.W. Tilanus, P.D. Siersema, H. Dekken, High-resolution array comparative genomic hybridization of chromosome 8q: evaluation of putative progression markers for gastroesophageal junction adenocarcinomas, Cytogenet. Genome Res. 118 (2–4) (2007) 130–137.
[25] E.C.H. Ho, M.E. Donaldson, Barry J Saville Detection of antisense RNA transcripts by strand-specific RT-PCR, Methods Mol. Biol. 630 (2010) 125–138.
[26] Z. Feng, et al., New preoperative nomogram using the centrality index to predict high nuclear grade clear cell renal carcinoma, Cancer Manag. Res. 11 (2020) 10921–10928.
[27] C. You, L. Jin, Q. Xu, B. Shen, X. Jiao, X. Huang, Expression of miR-21 and miR-138 in colon cancer and its effect on cell proliferation and prognosis, Oncol. Lett. 17 (2) (2019) 2271–2277.
[28] J.S. Ni, et al., MicroRNA-197-3p acts as a prognostic marker and inhibits cell invasion in hepatocellular carcinoma, Oncol. Lett. 17 (2) (2019) 2317–2327.
[29] T. Sjöblom, et al., The consensus coding sequences of human breast and colorectal cancers, Science 314 (5797) (2006) 268–274.
[30] A.D. D'Andrea, M. Grompe, The Fanconi anaemia/BRCA pathway, Nat. Rev. Cancer 3 (1) (2003) 23–34.
[31] K. Shostak, et al., NF-κB-induced KIAA1199 promotes survival through EGFR signaling, Nat. Commun. 5 (2014) 5232.
[32] P. Tarantino, et al., Evolution of low HER2 expression between early and advanced-stage breast cancer, Eur. J. Cancer 163 (2022) 35–43.
[33] D. Pe'er, S. Ogawa, O. Elhanani, L. Keren, T.G. Oliver, D. Wedge, Tumor heterogeneity, Cancer Cell 39 (8) (2021) 1015–1017.
[34] A.T. Beksac, D.J. Paulucci, K.A. Blu, S.S. Yadav, J.P. Sfakianos, K.K. Badani, Heterogeneity in renal cell carcinoma, Urol. Oncol. 35 (8) (2017) 507–515.
[35] S. Yalcin, S. Lacin, Impact of tivozanib on patient outcomes in treatment of advanced renal cell carcinoma, Cancer Manag. Res. 11 (2019) 7779–7785.
[36] H.T. Yang, R.H. Shah, D. Tegay, K. Onel, Precision oncology: lessons learned and challenges for the future, Cancer Manag. Res. 11 (2019) 7525–7536.
[37] A. Fire, S. Xu, M.K. Montgomery, S.A. Kostas, S.E. Driver, C.C. Mello, Potent and specific genetic interference by double-stranded RNA in Caenorhabditis elegans, Nature 391 (6669) (1998) 806–811.
[38] S.M. Elbashir, J. Harborth, W. Lendeckel, A. Yalcin, K. Weber, T. Tuschl, Duplexes of 21-nucleotide RNAs mediate RNA interference in cultured mammalian cells, Nature 411 (6836) (2001) 494–498.
[39] J. Shen, W. Zhang, R. Qi, Z.W. Mao, H. Shen, Engineering functional inorganic-organic hybrid systems: advances in siRNA therapeutics, Chem. Soc. Rev. 47 (6) (2018) 1969–1995.
[40] K.A. Schafer, The cell cycle: a review, Vet. Pathol. 35 (6) (1998) 461–478.
[41] C. Doglioni, P. Pelosio, L. Laurino, E. Macri, E. Meggiolaro, F. Favretti, M. Barbareschi, p21/WAF1/CIP1 expression in normal mucosa and in adenomas and adenocarcinomas of the colon: its relationship with differentiation, J. Pathol. 179 (3) (1996) 248–253.
[42] J.S. Lam, A. Breda, A.S. Belldegrun, R.A. Figlin, Evolving principles of surgical management and prognostic factors for outcome in renal cell carcinoma, J. Clin. Oncol. 24 (35) (2006) 5565–5575.
[43] A. Hwang, A. Maity, W.G. McKenna, R.J. Muschel, Cell cycle-dependent regulation of the cyclin B1 promoter, J. Biol. Chem. 270 (47) (1995) 28419–28424.
[44] B.V. Kallakury, S. Karikehalli, A. Haholu, C.E. Sheehan, N. Azumi, J.S. Ross, Increased expression of matrix metalloproteinases 2 and 9 and tissue inhibitors of metalloproteinases 1 and 2 correlate with poor prognostic variables in renal cell carcinoma, Clin. Cancer Res. 7 (10) (2001) 3113–3119.
[45] Y. Gao, et al., CXCL5/CXCR2 axis promotes bladder cancer cell migration and invasion by activating PI3K/AKT-induced upregulation of MMP2/MMP9, Int. J. Oncol. 47 (2) (2015) 690–700.
[46] C.X. Xiao, et al., ECHS1 acts as a novel HBsAg-binding protein enhancing apoptosis through the mitochondrial pathway in HepG2 cells, Cancer Lett. 330 (1) (2013) 67–73.